Stand-off detection of trace explosives via resonant infrared photothermal imaging

R. Furstenberg, C. A. Kendziora,[a] J. Stepnowski, S. V. Stepnowski, M. Rake, M. R. Papantonakis, V. Nguyen, G. K. Hubler, and R. A. McGill
U.S. Naval Research Laboratory, Code 6365, 4555 Overlook Avenue, SW, Washington, DC 20375, USA

(Received 22 August 2008; accepted 19 September 2008; published online 4 December 2008)

We describe a technique for rapid stand-off detection of trace explosives and other analytes of interest. An infrared (IR) laser is directed to a surface of interest, which is viewed using a thermal imager. Resonant absorption by the analyte at specific IR wavelengths selectively heats the analyte, providing a thermal contrast with the substrate. The concept is demonstrated using trinitrotoluene and cyclotrimethylenetrinitramine on transparent, absorbing, and reflecting substrates. Trace explosives have been detected from particles as small as 10 μm. © *2008 American Institute of Physics*. [DOI: 10.1063/1.3027461]

Motivated by homeland security and improvised explosive device concerns, explosives detection is an active area of research. One goal is to augment point detection with stand-off capability. For most applications, a stand-off technique should be eye and skin safe, provide rapid real-time analysis, and be adaptable to other types of threats. In this letter we demonstrate a resonant infrared (IR) photothermal approach that has the potential to meet these goals. In this approach, light of a specific IR wavelength is directed to the surface of interest[1] and the thermal response is viewed with an IR detector. Substances that resonantly absorb this wavelength will absorb light more efficiently than the rest of the surface, and the subsequent IR radiation provides a thermal contrast to the surrounding surface. As an optical technique, it is complementary to, but distinct from, other approaches in the literature,[2,3] including IR backscattering,[4] photothermal deflection spectroscopy,[5] Raman,[6] laser-induced breakdown spectroscopy,[7] coherent anti-Stokes Raman,[8] light detection and ranging,[9] photoacoustic,[10] cavity ringdown,[11] and terahertz[12] spectroscopy.

IR spectroscopy has long been utilized to identify chemical species based on absorption or reflection properties. In particular, the signature sequence of absorption bands is unique to each material, but certain trends emerge. Figure 1 shows the mid-IR transmission spectrum for humid air, 2,4,6-trinitrotolune (TNT) and cyclo-1,3,5-trimethylene-2,4,6-trinitramine (RDX). Because they share a common functional NO_2 group, these explosives exhibit similar absorption spectral features, including the band at 6.25 μm associated with the antisymmetric N–O stretch. Several other absorption features in common are noted in Fig. 1. In this letter, we emphasize this 6.25 μm wavelength region but the approach is also applicable to the other bands (and to other analytes of interest). 6.25 μm offers the advantage of being outside the detection range of most filtered IR detectors. 6.25 μm also falls within a narrow band where humid air is relatively transparent, allowing propagation over long distances.

The transient thermal response of a small particle (p) on a substrate (s) [Fig. 2(a)] to a laser pulse can be described by the following system of equations:

$$\rho_p c_p V_p \frac{\partial T_p(t)}{\partial t} = \dot{q} - h[T_p(t) - T_s(0,0,t)],$$

$$\rho_s c_s \frac{\partial T_s(r,z,t)}{\partial t} = K_s \nabla^2 T_s(r,z,t) + h[T_p(t) - T_s(0,0,t)],$$

$$\dot{q} = \begin{cases} IQ_{\text{abs}}(\lambda, R_p)\pi R_p^2, & t \le t_{\text{laser}} \\ 0, & t > t_{\text{laser}}, \end{cases} \quad (1)$$

where V_p is the particle volume, $Q_{\text{abs}}(\lambda, R_p)$ is the wavelength and particle size dependent effective absorption cross section,[13] I is the laser irradiance (W/m^2), R_p is the particle radius, h is the contact thermal resistance, and ρ, c, and K are the density, heat capacity, and thermal conductance. The particle is loosely attached to the substrate that is modeled through thermal contact resistance. A uniform temperature distribution within the particle can be assumed due to its small size. Convective heat loss is omitted in Eq. (1) as it was empirically shown (by introducing airflow over the substrate) that convection does not affect the laser heating process.

The experimental apparatus [Fig. 2(b)] utilizes a commercial quantum cascade laser (QCL) (Daylight Solutions), which is tunable in continuous wave (cw) mode from 6.1 to

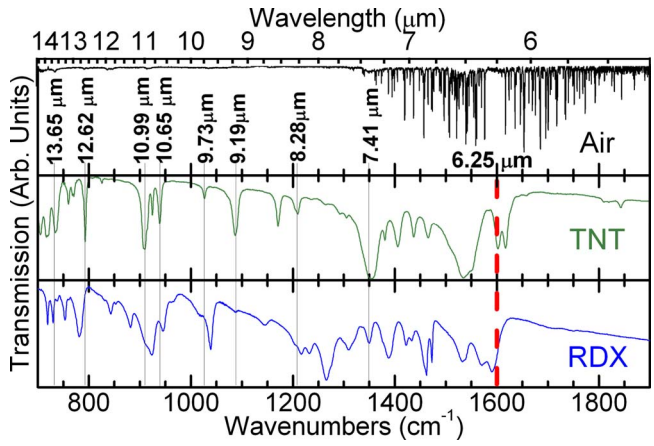

FIG. 1. (Color online) IR transmission spectra of air, TNT, and RDX. Shared absorption bands are highlighted.

[a]Electronic mail: kendzior@ccs.nrl.navy.mil.

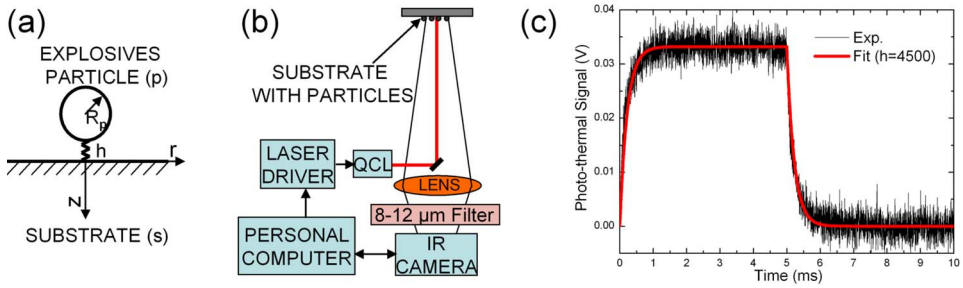

FIG. 2. (Color online) (a) The model used in Eq. (1). (b) The experimental setup. (c) Transient thermal profile of carbon powder (mesh −100) on a copper substrate illuminated with a laser ($I \approx 80$ mW/cm^2, $\lambda = 785$ nm) at 1 m stand off. Signal recorded with a LN cooled MCT detector.

6.4 μm. This laser produces up to 30 mW cw with a spectral width of ≈ 1 cm^{-1}. A variety of pure analytes on different substrates with different amounts and morphologies was tested. The optical configuration utilizes a nearly collimated excitation beam colinear with the collection axis. IR collection is done with a 100 mm ($f/1$) lens (Ophir) after the thermal signal is passed through an 8–12 μm filter. Detection has been performed using a LN2 cooled mercury-cadmium-telluride (MCT) single element detector (Infrared Associates) and an uncooled microbolometer array (FLIR, Inc.: 320×240 pixels, 38 μm pitch, NETD=85 mK, 30 frames/s). The difference signal (laser on versus laser off) is the relevant parameter. This is done by either pulsing/chopping the laser beam (MCT) or subtracting images (array detector). We observe temperature differences of up to a few degrees (in $t=100$ ms) depending on the thermal properties of the substrate. We have demonstrated the technique on three limiting substrate cases: IR transparent, IR absorbent, and IR reflecting/scattering.

Figure 2(c) shows a typical thermal profile of carbon particles on a copper sheet heated by a 785 nm laser diode. The particles in this test sample were made from carbon because unlike explosives, they are easily prepared yet provide a relatively good model for explosives particles. Trace explosives samples were prepared by drying out solutions on substrates. This process tends to yield better thermal contact with the substrate, thereby making analytes that heat less and are therefore harder to detect than explosives residues likely to be found in the field.[14] Depending on the thermal properties of the substrate and the particle, typical thermal relaxation (i.e., cooling) times (τ_{cool}) can range from <1 ms for particles on metallic substrates to several tens of milliseconds for ones on insulating substrates. A rough estimate of the temperature rise can be given by $\Delta T \approx 3I\tau_{\text{cool}}Q_{\text{abs}}(\lambda, R_p)/4\rho_p c_p R_p$. For example, a 5 μm RDX particle ($\rho=1700$ kg/m^3, $c=1250$ J/kg K)[15] illuminated for 10 ms ($\approx\tau_{\text{cool}}$) with a 10 mm diameter 50 mW laser beam tuned to an absorption band and assuming full absorption ($Q_{\text{abs}}=1$) is expected to heat by ≈ 1 K. This is more than adequate as modern IR technology has a detection limit of ≈ 20 mK. This rapid response enables the photothermal technique to quickly distinguish analytes of interest.

The photothermal signal from the region around the particle is given by $\approx \pi R_p^2 \int_{\lambda_1}^{\lambda_2} \{d\lambda \varepsilon_p(\lambda) H(\lambda, T_p) + \varepsilon_s(\lambda) H(\lambda, T_s^{\text{avg}})\}$, where $\varepsilon_p(\lambda)$ and T_p are the emissivity and temperature of the particle, $\varepsilon_s(\lambda)$ and T_s^{avg} are the emissivity and average temperature (under particle) of the substrate, and $H(\lambda, t)$ is the black body radiation. It is important to note that the emissivity of chemical compounds (including explosives) is highly wavelength dependent and is directly related to the absorption coefficient (in accordance with Kirchhoff's law). We use the 8–12 μm air transparency window to take advantage of the higher emissivity values of RDX and TNT in this band.

Figure 3 illustrates the resonant photothermal technique using TNT and RDX analytes deposited on an IR transparent polypropylene film. As the QCL wavelength is tuned across the N–O absorption band, the analytes are selectively heated. The spot size, illustrated by the dashed circle in Fig. 3, is ≈ 10 mm. The laser power varied from 3 to 18 mW, and the image intensities were normalized by this factor. This sequence of images demonstrates the selectivity of the photothermal technique, even between types of explosives. Figure 4(a) shows a thermal image of TNT particles on a stainless steel substrate. Figure 4(b) shows the differential thermal image (laser on minus laser off) of the identical scene. This was measured at 1 m stand off using 20 mW of 6.25 μm light into a 10 mm spot. Individual particles of sizes 10–100 μm diameter (0.8–800 ng) can be observed. The temperature difference is ≈ 1 °C for the large grain seen in both images.

For photothermal detection in general, the fundamental limits to stand-off distance depend on the laser power and

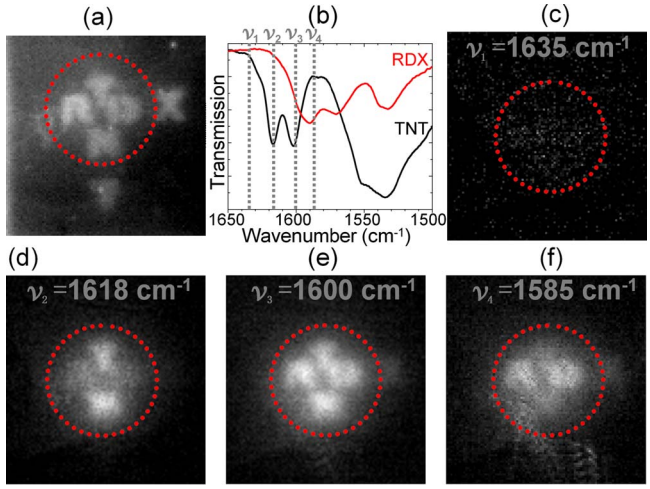

FIG. 3. (Color online) Illustration of resonant photothermal heating. Letters "RDX" and "TNT" were written on a polypropylene film using solution of the explosives. (a) Result of nonselective heating using a heat gun. (b) IR spectrum of RDX and TNT showing resonances. (c) Laser heating with off-resonance wavelength. (d) Laser heating on resonance with TNT only. (e) Laser heating on resonance with RDX and TNT. (f) Laser heating on resonance with RDX only.

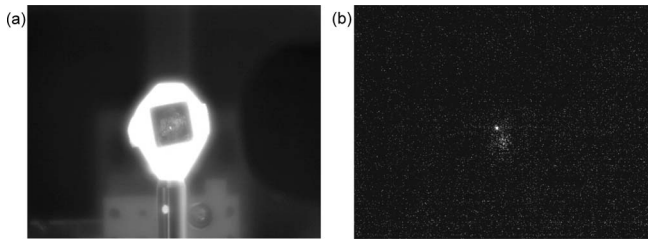

FIG. 4. (a) Raw thermal image of TNT particles on a stainless steel substrate. (b) Differential image (laser on minus laser off). Individual particles of sizes 10–100 μm diameter can be observed (1 m stand off, 20 mW, 6.25 μm, 10 mm spot).

divergence as well as the collection efficiency and detector sensitivity. The ANSI standard maximum permissible exposure (MPE) for eye safety in this IR wavelength range is 0.1 W/cm^2 cw.[16] A beam that starts out at the eye-safe level will drop in intensity due to divergence ($\propto \lambda/\text{diameter}$) and atmospheric absorption. At the eye-safe MPE, surface particles heat by up to a few °C. While a few degrees of change is observed at stand off, it becomes difficult to resolve small spatial features. For example, using our 100 mm focal length lens, at 26.3 m a 1 cm diameter object will image to the 38 μm pixel size of our array. The collected thermal signal should decrease with distance by $1/R^2$.

"Black" materials that strongly absorb all wavelengths pose a possible interference for this technique. For this reason, it is critical to use a reference excitation wavelength that is off resonance, thereby limiting the false positive signal. We have demonstrated this with analyte on an absorbing black plastic. In the case of a black substrate, the resonant absorption by analytes of interest on the surface can be further distinguished by temporally resolving the heating profile. The particles will tend to heat first with a shorter time constant than the substrate. In addition, it is possible to exploit the spectral signatures of the thermal signal itself since by Kirchhoff's law the emission spectrum matches the absorption spectrum. Thus, spectral filters on the collection optics could enhance the selectivity.

The IR excitation wavelength could be shifted to couple to nitrate explosives, such as ammonium nitrate fuel oil or urea nitrate. These nitrate explosives share the NO_3- ionic species, which gives a strong N–O absorption band at 7.3 μm. Similarly the resonant IR technique could be applied to other classes of explosives, including peroxide based and those not yet discovered. It could also be adapted to nonexplosive materials of interest, such as chemical warfare agents or drugs of abuse.

In conclusion, resonant IR photothermal imaging is a promising technique for rapid selective stand-off detection of trace explosives. It has been demonstrated using RDX and TNT traces on a wide range of substrates including transparent, reflecting, and absorbing. The photothermal signal is largest on substrates with low thermal conductivity. Further development of the technique is ongoing, including testing it outdoors as a function of temperature, humidity, wind, dirt, and ambient light. We have also developed a single channel detection modality not requiring an imaging array. To increase the selectivity and sensitivity, we are also utilizing multiwavelength and sweeping wavelength approaches.

The authors gratefully acknowledge support from ONR/NRL (61153N, MA022-06-4G). Part of this work was supported under OSD/RRTO (Grant No. DRE-3826-777). This research was performed while R.F. held a National Research Council Research Associateship Award at the U.S. Naval Research Laboratory.

[1] D. M. Bubb, J. S. Horwitz, R. A. McGill, D. B. Chrisey, M. R. Papantonakis, R. F. Haglund, Jr., and B. Toftmann, Appl. Phys. Lett. **79**, 2847 (2001).
[2] D. S. Moore, Rev. Sci. Instrum. **75**, 2499 (2004).
[3] C. A. Munson, J. L. Gottfried, F. C. De Lucia, Jr., K. L. McNesby, and A. W. Miziolek, Report No. ARL-TR-4279 (2007); http://www.arl.army.mil/arlreports/2007/ARL-TR-4279.pdf
[4] F. Fuchs, Ch. Wild, Y. Rahmouni, W. Bronner, B. Raynor, K. Köhler, and J. Wagner, Proc. SPIE **6739**, 673904 (2007).
[5] C. W. Van Neste, L. R. Senesac, D. Yi, and T. Thundat, Appl. Phys. Lett. **92**, 134102 (2008).
[6] M. L. Lewis, I. R. Lewis, and P. R. Griffiths, Appl. Spectrosc. **58**, 420 (2004).
[7] F. C. DeLucia, Jr., A. C. Samuels, R. S. Harmon, R. A. Walters, K. L. McNesby, A. LaPointe, R. J. Winkel, Jr., and A. W. Miziolek, IEEE Sens. J. **5**, 681 (2005).
[8] H. Li, D. A. Harris, B. Xu, P. J. Wrzesinski, V. V. Lozovoy, and M. Dantus, Opt. Express **16**, 5499 (2008).
[9] C. Bauer, J. Burgmeier, C. Bohling, W. Schade, and G. Holl, in *Stand-off Detection of Suicide Bombers and Mobile Subjects*, edited by H. Schubert and A. Rimski-Korsakov (Springer, New York, 2006), pp. 127–133.
[10] C. W. Van Neste, L. R. Senesac, and T. Thundat, Appl. Phys. Lett. **92**, 234102 (2008).
[11] M. W. Todd, R. A. Provencal, B. A. Paldus, A. Kachanov, K. L. Vodopyanov, M. Hunter, S. L. Coy, J. I. Steinfeld, and J. T. Arnold, Appl. Phys. B: Lasers Opt. **75**, 367 (2002).
[12] M. C. Kemp, C. Baker, and I. Gregory, in *Stand-off Detection of Suicide Bombers and Mobile Subjects*, edited by H. Schubert and A. Rimski-Korsakov (Springer, New York, 2006), pp. 151–165.
[13] C. F. Bohren and D. R. Huffman, *Absorption and Scattering of Light by Small Particles* (Wiley-VCH, Weinheim, 2004), p. 72.
[14] J. R. Verkouteren, J. Forensic Sci. **52**, 335 (2007).
[15] Department of the Army, *Military Explosives* Army Technical Manual TM 9–1300–214 (Headquarter of the Army, Washington D.C., 1984).
[16] *ANSI Standard 2136.1* (Laser Institute of America, Orlando, 2007), Table 5a.